A Letters Journal Exploring the Frontiers of Physics

October 2009

EPL, **88** (2009) 24001
doi: 10.1209/0295-5075/88/24001

www.epljournal.org

Experimental model of the interfacial instability in aluminium reduction cells

A. Pedchenko[1(a)], S. Molokov[1], J. Priede[1], A. Lukyanov[2] and P. J. Thomas[3]

[1] *Applied Mathematics Research Centre, Coventry University - Priory Street, Coventry CV1 5FB, UK, EU*
[2] *Department of Mathematics, University of Reading - Whiteknights, PO Box 220, Reading RG6 6AX, UK, EU*
[3] *Fluid Dynamics Research Centre, School of Engineering, University of Warwick - Coventry, CV4 7AL, UK, EU*

received 10 August 2009; accepted in final form 2 October 2009
published online 3 November 2009

PACS 47.65.-d – Magnetohydrodynamics and electrohydrodynamics
PACS 52.30.Cv – Magnetohydrodynamics (including electron magnetohydrodynamics)

Abstract – A solution has been found to the long-standing problem of experimental modelling of the interfacial instability in aluminium reduction cells. The idea is to replace the electrolyte overlaying molten aluminium with a mesh of thin rods supplying current down directly into the liquid metal layer. This eliminates electrolysis altogether and all the problems associated with it, such as high temperature, chemical aggressiveness of media, products of electrolysis, the necessity for electrolyte renewal, high power demands, etc. The result is a room temperature, versatile laboratory model which simulates Sele-type, rolling pad interfacial instability. Our new, safe laboratory model enables detailed experimental investigations to test the existing theoretical models for the first time.

Copyright © EPLA, 2009

Introduction. – Overcoming magnetohydrodynamic (MHD) instabilities in aluminium reduction cells is a problem of enormous industrial importance [1]. This is not surprising as current production facilities consume about 2% of the entire electricity generated worldwide, which translates into about 10 billion US dollars annually [2]. Thus the efficiency of the process of aluminium smelting has considerable economic dimension.

Aluminium is produced in rows of about 100 shallow baths or cells with horizontal dimensions of 4–5 m by 10–16 m each by passing an electric current of between 150 and 500 kA through a mixture of alumina (Al_2O_3) and cryolite (sodium aluminium fluoride) (fig. 1). The electric current flows vertically down from the carbon anodes at the top of the cell to the carbon cathode at the bottom, melting both alumina and cryolite by means of Joule heating. As a result of very complex thermo-, electro-, hydro-, magnetohydro-dynamic, and electrochemical processes involving consumption of carbon from anodes and accompanying CO_2 and perfluorocarbon gas emissions, a two-fluid layer is formed, up to 35 cm deep. The fluid on top, about 4–5 cm thick, is an electrolyte with very poor electrical conductivity of $\sigma_c \approx 200\,(\Omega\mathrm{m})^{-1}$ while the fluid below is a slightly heavier molten aluminium with high conductivity of $\sigma_a \approx 3 \times 10^6\,(\Omega\mathrm{m})^{-1}$. Both are kept at about 960 °C.

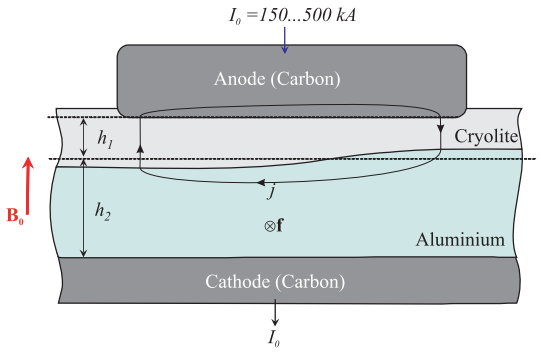

Fig. 1: (Colour on-line) Schematic diagram of the aluminium smelting process.

The interface between the electrolyte and the liquid metal may become unstable to MHD waves if parameters of the process rise above or fall below certain thresholds. The key to the mechanism of instability, suggested first by Sele [3], is the MHD interaction of the horizontal component of the disturbance electric current $\mathbf{j}$ (see fig. 1), which flows mainly in highly conducting aluminium layer with the vertical component of the background field B_0. The Lorentz force $\mathbf{f} = \mathbf{j} \times \mathbf{B}_0$ (see fig. 2) drives the metal

(a) E-mail: a.pedcenko@coventry.ac.uk

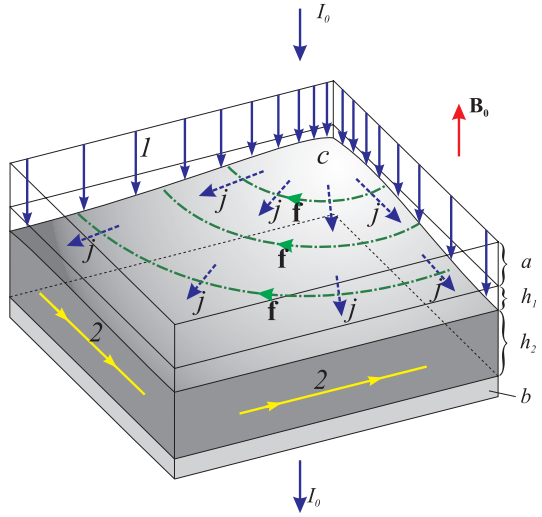

Fig. 2: (Colour on-line) Schematic diagram of the instability mechanism; a: anode, b: cathode, c: deformed liquid metal surface, h_1: cryolite, h_2: molten aluminium, 1: vertical current entering aluminium, j: horizontal disturbance current in the aluminium layer, **f**: the direction of the Lorentz force, 2: the direction of the rotating wave.

into horizontal motion (position 2) resulting in a rotating interface, which under certain conditions may become unstable. The background magnetic field is an unwanted side effect of the bus bars supplying the current to the cells and cannot be eliminated entirely.

The electrodynamic role of the electrolyte is simple: to pass the current vertically down into the aluminium (fig. 2, position 1) for the following obvious reason. The electrolyte is a very poor conductor, which implies that the electric current flows in the direction of least resistance, mainly vertical. The electric potential difference across the electrolyte layer results in many undesirable accompanying features of electrolysis, such as high power demands and generation of gases and harmful products of chemical reactions.

Direct measurements of fluid flow in the cells are very limited due to high temperature and chemical aggressiveness of the melts. Two types of measurements are widely used. The first one is the iron rod method, whereby a rod is dipped into aluminium and the intensity of the fluid flow is judged by the rate of dissolution of the rod over a prolonged period of time [4]. The other method consists of measuring the global potential difference between the anodes and the cathode, which gives the variation of the total resistance of the cell with time, and thus enables conclusions regarding the global unsteady fluid flow.

Needless to say that neither of these methods is precise. It is thus not surprising that studies of the instabilities have been of theoretical nature, see the review in [5], suggesting various mechanisms and flow models, but none of these models has yet been verified experimentally. Thus the necessity for a safe, cold model of the cell involving non-aggressive fluids cannot be overestimated.

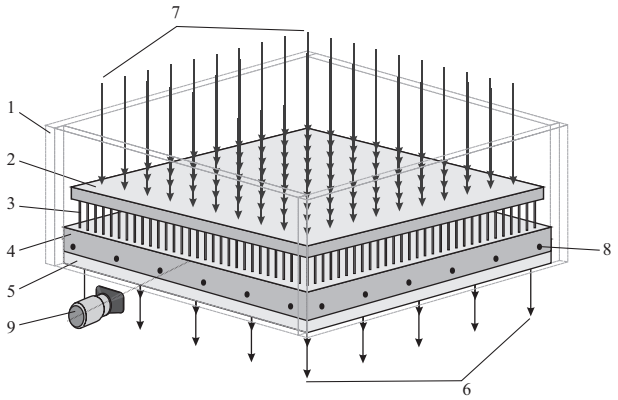

Fig. 3: Sketch of the experimental model. 1: Lexan side walls, 2: copper anode plate, 3: 900 stainless-steel electrodes, 4: liquid metal, In-Ga-Sn, 5: stainless-steel cathode plate, 6: wires collecting current from the cathode (25 in total), 7: wires supplying current to the anode (100 in total), 8: electric potential probes, 9: CCD camera for tracking the elevation of the liquid metal.

Here we present a solution for experimental modelling that does not involve the use of an electrolyte and that consequently eliminates undesired electrolysis altogether allowing to create a low-temperature versatile laboratory model which reproduces Sele-type of instability. In this model the electrolyte is replaced by a system of thin vertical rods connected to the anode plate and dipped directly into the liquid metal. This fulfils the electrodynamic role of the electrolyte to conduct current vertically down into the liquid metal but at the same time eliminates all the problems related to high temperatures, aggressiveness of the electrolyte, products of the electrolysis, electrolyte renewal, high power demands, etc.

Experimental setup. – The experimental cell depicted schematically in fig. 3 represents a container with square horizontal cross-section with dimensions $30 \times 30\,\mathrm{cm}^2$. The box has 15 cm high, electrically insulating, polycarbonate side walls and a stainless-steel bottom. It is filled with a thin layer of metal, In-Ga-Sn, as a substitute for aluminium, which remains liquid at room temperature. This type of liquid metal is widely used in MHD experiments.

The electric current is supplied to the layer from the anode, located at the top of the cell. The anode is a 15 mm thick copper plate with 900 electrodes made of stainless steel, which are 40 mm long and 2 mm in diameter. The electrodes are inserted into the bottom surface of the anode plate and distributed uniformly with a 10 mm pitch. Being directly immersed into the liquid metal with their tips, these electrodes conduct the electric current between the nearly equipotential anode plate and the liquid metal. The immersion depth of the electrodes may be varied by lowering or lifting the anode plate. The surface of the liquid metal is free to move along the electrodes in the gap with the anode plate.

The effective conductivity of the system of steel electrodes is 75 times lower than that of the same height of liquid metal. Thus the electrodynamic properties of the electrodes are similar to those of the electrolyte. If the liquid metal rises in some area of the cell, the length of the electrodes (and hence their resistance) in that region reduces, causing higher current in that area of liquid metal. For cell areas with lower level of liquid metal the resistance of the electrodes becomes higher which results in lower current. In other words, the interface shape is driving non-homogeneity of the anode current, which enters the liquid metal and redistributes horizontally within the liquid metal layer before entering the steel bottom with lower electrical conductivity.

The space between the anode plate and the liquid metal surface has been filled with a weak ($\sim 3\%$) HCl water solution to minimise oxidation of the liquid metal surface, to avoid liquid metal sticking to the side walls during sloshing, and to provide some cooling for the anode electrodes in case of the electric contact interruption between some of the electrodes and the liquid metal. This second liquid, however, does not conduct electric current, but may serve to minimise density difference between the fluids thus making interfacial waves less stable.

As is known from linear stability studies [3,5,6], the instability occurs once the value of the dimensionless parameter

$$\beta = \frac{I_0 B_0}{g \Delta\rho h_1 h_2} \tag{1}$$

exceeds a certain threshold β_c, which depends on the geometry of the cell and dissipation in the system. In the above I_0 is the anode current, B_0 is the external magnetic field, $\Delta\rho = \rho_2 - \rho_1$ is density difference between the liquid metal and electrolyte, h_1 and h_2 are the thicknesses of the electrolyte and liquid metal layers, respectively (in the experiment h_1 is the length of the electrodes and ρ_1 is the density of the HCl-water solution). For the square cell used in the experiment, linear stability analysis predicts $\beta_c = 0$. Unfortunately, the analysis does not take into account the dissipation, which is significant and includes magnetic damping.

To destabilize the system we tried to maximize the β value by maximizing the product $I_0 B_0$ for the disturbance Lorentz force to overcome damping.

The maximum anode current in the experiment has been 1.8 kA, which allows to achieve the maximum current density in the experiment of 2.2 A/cm^2. This is more than 4 times higher than that in real cells.

The background magnetic field is generated by two induction coils switched in parallel (not shown in fig. 3) surrounding the cell. The cell is placed in the gap between these two coils, in the region where the magnetic field has only the vertical component with non-uniformity over the horizontal cross-section of the liquid metal of $\sim 5\%$ and the absolute value of up to 0.1 T. The maximum magnetic field is 20 times higher than that in real cells.

Measurement techniques. – To register oscillations in the liquid metal two measurement techniques have been used: I) recording the distribution of the electric potential ϕ at the sidewalls along the perimeter of the cell (fig. 3, position 8) and II) tracking the elevation of the liquid metal at a fixed point along the cell perimeter with CCD camera (fig. 3, position 9).

Twenty-four electric potential probes installed in the side walls of the cell, 10 mm above the bottom, are equally distributed along the perimeter to measure instantaneous values of ϕ at these locations with reference to a point at the centre of the cell. The electric potential at the sidewalls is related to the horizontal current by means of Ohm's law, $\mathbf{j} = -\sigma_a \nabla\phi$, where ∇ is the gradient in the horizontal plane. Thus ϕ gives information about the strength of the disturbance Lorentz force $\mathbf{f}$ at the sidewalls. The measurements of the sidewall potential also provide qualitative information on the overall behaviour of the liquid metal surface since ϕ is related to the elevation of the interface [6,7].

The second measurement technique used in the experiment is high-resolution video recording of the liquid metal elevation in the middle of a sidewall (fig. 3, position 9) with a frame rate of 30 fps. This data provides quantitative information about the amplitude of the liquid metal height oscillations, waveform, frequency and spectrum.

Results. – The procedure of the experiments has been as follows: first, the anode was lowered for the electrodes to immerse into the liquid metal. Next, the anode current was switched on to the maximum value of 1.8 kA and after that a vertical magnetic field was switched on.

Switching on the magnetic field, provided the latter was strong enough, generated an initial surface disturbance, which rapidly evolved into a rotating wave of a relatively large amplitude. For $\mathbf{I}_0$ and $\mathbf{B}_0$ directed opposite to each other, the wave rotated in the counter-clockwise direction when viewed from the top. Changing the direction of $\mathbf{B}_0$ or $\mathbf{I}_0$ to the opposite changed the direction of rotation. Once the instability had been developed, the current was lowered to the desired value.

This procedure was done to overcome capillary effects, possible contact resistance at the electrodes and magnetic damping, which require more detailed studies. Since surface tension is very high in liquid metals, wetting of the electrodes by the metal prevents system response to the perturbations with amplitude lower than capillary length (a few mm).

If the amplitude of the wave was larger than the depth of the electrodes' immersion, it resulted in the loss of the electric contact between the electrodes and the lowered parts of the interface. This generated even more non-uniform I_0 distribution along the metal surface, and, subsequently, even higher horizontal disturbance current.

The experimental values of β computed according to (1) for which the rotating wave was observed, lay in the range of 0.03–8.

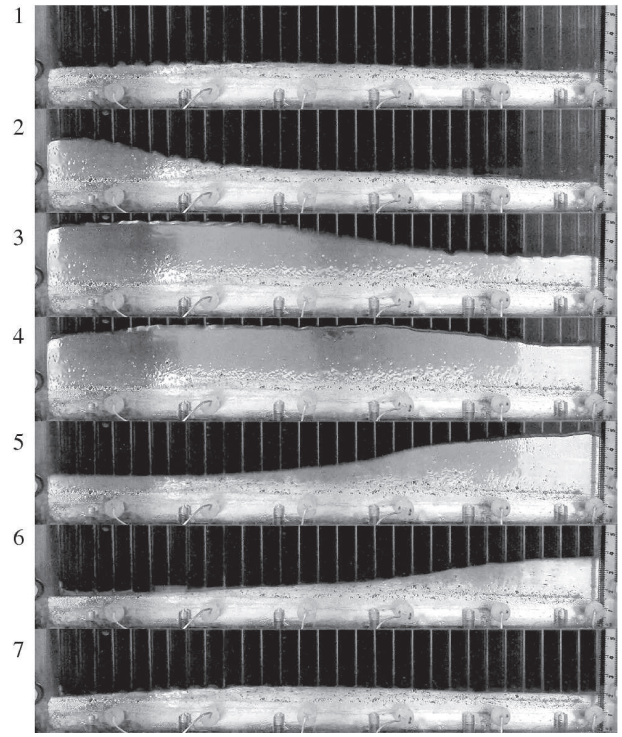

Fig. 4: Sequence of video frames showing passing liquid metal wave along a sidewall of the cell; the time step between the frames is 0.2 s; the wave period is 1.2 s; $h_2 = 35$ mm, $I_0 = 1.2$ kA, $B_0 = 100$ mT; the vertical scale is 55 mm per frame.

The sequence of video frames in fig. 4 demonstrates a high-amplitude wave passing along one of the sidewalls of the cell.

Figure 5 provides time history of the measured electric potential along the sidewalls. It clearly represents a wave rotating along the perimeter of the cell with a single frequency. The obtained map of the potential correlates very well with optical observations of liquid metal interface oscillations. At low amplitudes of the wave, its propagation rate measured for different liquid metal heights, h_2, is slightly above the phase speed of the interfacial gravity waves for two immiscible liquids given by [5]

$$c_0 = \sqrt{\frac{g\Delta\rho}{\frac{\rho_1}{h_1} + \frac{\rho_2}{h_2}}}, \qquad (2)$$

as predicted by linear stability theories (see, *e.g.*, [6]).

The amplitude of the wave varies in a wide range of 3–50 mm increasing with the anode current I_0 and the magnetic field B_0. The frequency of the wave observed in the experiment varies with the thickness h_2 of the liquid metal layer in the range of 0.5–0.9 Hz for $h_2 = 10$–45 mm.

The amplitude, h^*, of the liquid metal surface oscillations is found to depend linearly on the anode current, I_0, as shown in fig. 6 for several values of the external magnetic field B_0. One can see that for increasing induction of the magnetic field, up to about 50 mT the surface oscillations increase. For $B_0 > 50$ mT there is almost no dependence of h^* on B_0. This implies that the magnetic

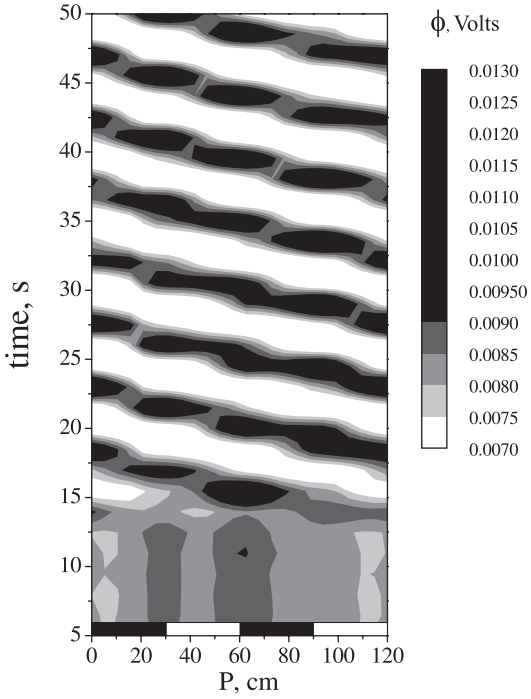

Fig. 5: Time-spatial distribution of the electric potential along the perimeter of the cell P; the initial stage (5–15 s) corresponds to the onset of the wave; black and white bars at the bottom of the graph show the sidewalls of the cell.

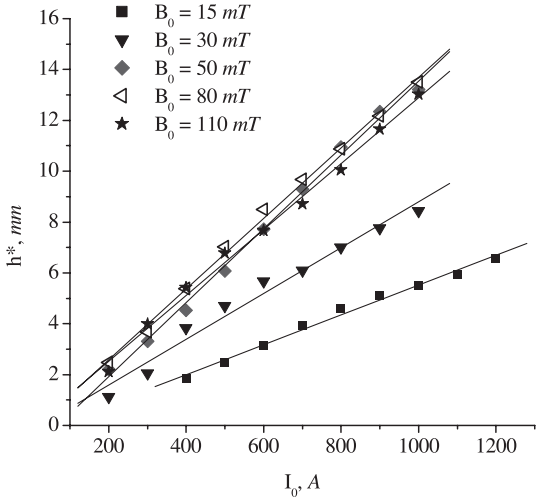

Fig. 6: RMS value of interface fluctuations h^* *vs.* current I_0.

damping at higher B_0 values compensates the destabilizing Lorentz force **f** suppressing further growth of the wave amplitude.

Besides the anode current and the vertical magnetic-field strengths, the amplitude of the wave depends on the thickness of the liquid metal in the cell. It is higher for lower levels of the liquid metal.

Conclusions. – A solution has been found for the long-standing problem of experimental modelling of the MHD instabilities in aluminium reduction cells. The idea is to

replace the electrolyte overlaying molten aluminium with a mesh of thin conducting electrodes dipped directly into the liquid metal. This fulfils the electrodynamic role of the electrolyte to pass the electric current down into the metal. At the same time this eliminates all the undesirable features of electrolysis altogether.

The facility has been successfully used to reproduce Sele-type of instability. This opens a way to more detailed experimental studies and to testing existing theoretical models [5]. These have never been verified owing to unavailability of an appropriate experimental laboratory model.

* * *

This work has been performed within the Aluminium Smelter Project No. 2005-3-2723-7 funded by Carbon Trust (UK), Rio Tinto Alcan, Coventry University and University of Warwick.

REFERENCES

[1] Moffatt H. K., *Reflections on magnetohydrodynamics,* in *Perspectives in Fluid Dynamics. A collective introduction on current research*, edited by Batchelor G., Moffatt H. K. and Worster M. G. (Cambridge University Press, Cambridge) 2000, Chapt. 7, pp. 347–391.

[2] Davidson P. A., *Mater. Sci. Technol.*, **16** (2000) 475.

[3] Sele T., *Light Met.*, **7–24** (1977) 313.

[4] da Mota G. and Blasques J., *Process Improvements to Raise the Line Current at Albras*, in *Light Metals 2004, Proceedings of 2004 TMS Annual Meeting* (TMS) 2004, pp. 185–190.

[5] Gerbeau J.-F., Bris C. L. and Lelievre T., *Mathematical Methods for the Magnetohydrodynamics of Liquid Metals* (Oxford University Press) 2006, Chapt. 6, pp. 233–302.

[6] Bojarevics V. and Romerio M., *Eur. J. Mech. B - Fluids*, **13** (1994) 33.

[7] Lukyanov A., El G. and Molokov S., *Phys. Lett. A*, **290** (2001) 165.